

P10.6 CHARACTERISTICS OF VERTICAL PROFILE OF RAINFALL PARAMETERS IN BAIU FRONTAL RAINFALL USING 2D-VIDEO DISTROMETER, COBRA, AND 400MHz WIND PROFILWER

Katsuhiro NAKAGAWA^{1,2}, Yukari SHUSSE², Yasushi KITAMURA³, and Robert MENEGHINI⁴

¹GEST/UMBC, Greenbelt, Maryland, USA

² National Institute of Information and Communications Technology, Japan

³KAIJO SONIC Corporation, JAPAN

⁴NASA/GSFC, Greenbelt, Maryland, USA

1. INTRODUCTION

To improve the accuracy of rainfall intensity and rain retrieval algorithms from space-borne radars (TRMM/PR and GPM/DPR), radiometers and ground-based radars, the vertical profile of the raindrop size distribution, is very important (T. Iguchi et. al. 2003, C. Kummerow et. al. 2001, K. Aonashi and G. Liu 2000).

Intensive field observations for subtropical precipitation using COBRA (C-band polarimetric radar), 400-MHz Wind Profiler (400-MHzWPR), and two types of ground-based disdrometer were carried out in June 2006 at Okinawa Island, Japan. These instruments are part of the Okinawa Sub-tropical Environment Remote Sensing Center, operated by the National Institute of Information and Communication Technology (NICT). The ground-based DSD was observed by a 2D-Video distrometer and a Joss-type disdrometer. Vertical profiles of the DSD were estimated from Doppler spectra observed by the 400MHz WPR. In 2004, COBRA and 2D-Video Distrometer data were used to analyze the vertical variation of rainfall for different rainfall types. The results show that in convective rainfall, vertical variations of the polarimetric parameter (ZDR and Do) are large (Nakagawa et. al 2005).

In this study, we analyzed the vertical characteristics of rainfall parameters for stratiform and convective rain types.

2. OBSERVATION

Intensive field observations for subtropical precipitation using COBRA (C-band polarimetric radar), 400-MHz Wind Profiler (400-MHzWPR) (K. Nakagawa et al., 2003, Adachi et al., 2001), and two types of ground-based disdrometer were carried out in June 2006 on the main island of Okinawa, Japan. Fig. 1

shows an outline of the intensive field observations.

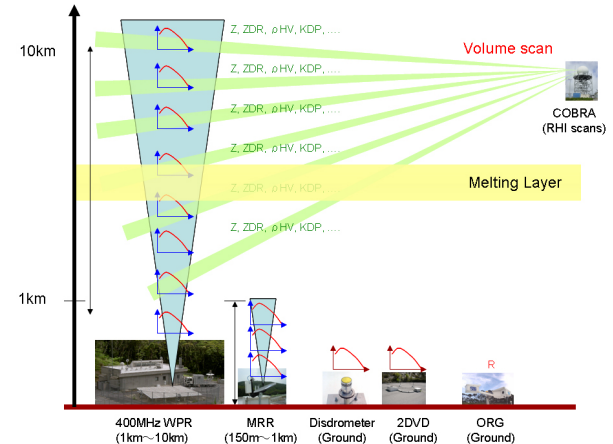


Fig. 1 Outline of the intensive field observations. The elevation angles of the PPI scans were from 0.5° to 20.5°.

At the NICT Ogimi facility site, the 400-MHz WPR performed synchronous observation with the COBRA system. Ground-based measurements of the rain drop size distribution were obtained each minute by a Joss-type disdrometer and a 2D-Video-Distrometer (2DVD). The rainfall intensity was also observed each minute with a tipping-bucket rain gauge and an optical rain gauge. COBRA was operated with 14 plan position indicator (PPI) and one range height indicator (RHI) scan every 6 minutes. The azimuth angle of the RHI was set at 330°. The RHI did not pass over the Ogimi site.

The 400-MHz WPR is able to observe simultaneously the atmospheric turbulence echo and the echo from precipitation. Therefore, by analyzing the echo power spectrum of the received signal, the rain drop size distribution can be estimated for which the effects of wind speed, the intensity of atmospheric turbulence, and background winds have been removed. Several methods have been proposed to estimate DSD from the UHF/VHF Wind Profiler data (e.g. K. Wakasugi et al., 1986, Sato et al., 1990). In this study, the DSD

*Corresponding author address:

Katsuhiro NAKAGAWA, GEST/UMBC, NASA/Goddard Space Flight Center, Greenbelt, Maryland 20771 USA; e-mail: katsu@neptune.gsfc.nasa.gov

below the melting layer observed by the 400-MHz WPR is basically retrieved by a non-parametric method (T. Kobayashi and A. Adachi, 2005). As the primary observation target of 400-MHz WPR is atmospheric turbulence, the receivers are sometimes saturated for rainfall observation. Therefore, a calibration factor for the 400-MHz WPR is used that is obtained by a comparison with the radar reflectivity of COBRA (Y. Kitamura et al., 2003).

3. OBSERVATION RESULTS

3.1 DSD parameter estimation method

The data were used to analyze the vertical variations of rainfall parameters that include raindrop size distribution (DSD), mass weighted drop diameter (D_m), normalized number concentration (N_0^*), radar reflectivity (Z), differential reflectivity (ZDR), and correlation coefficient (ρ_{HV}). The radar ZDR, and D_m were also derived from the 400-MHz WPR.

The rain drop size distribution is assumed to be given by the gamma distribution (gamma model),

$$N(D) = N_0 D^\mu \exp(-\Lambda D) \quad (1)$$

where D is the drop diameter, N_0 , μ , and Λ are the parameters of the gamma model. The x th moment of DSD, M_x , is expressed as (Ulbrich, 1983, T. Kozu and K. Nakamura, 1991)

$$M_x = \int D^x N(D) dD. \quad (2)$$

N_0^* and D_m can be expressed in terms of the moments by:

$$D_m = \frac{\int D^4 N(D) dD}{\int D^3 N(D) dD} = \frac{M_4}{M_3} \quad (3)$$

and

$$N_0^* = \frac{4^4}{\pi \rho_w} \cdot \frac{LWC}{D_m^4}. \quad (4)$$

LWC is the liquid water content and is defined by

$$LWC = \frac{\pi \rho_w}{6} \int D^3 N(D) dD = \frac{\pi \rho_w}{6} M_3. \quad (5)$$

For a gamma model of Eq. (1), Λ and μ are given by

$$\Lambda = \frac{\mu + 4}{D_m} \quad (6)$$

and

$$\mu = \frac{11G - 8 + \sqrt{G(G + 8)}}{2(1 - G)}, \quad (7)$$

where G is

$$G = \frac{M_4^3}{M_3^2 M_6}. \quad$$

3.2 Rainfall type classification

To characterize the vertical variations in the rainfall parameters for the various rainfall types during the Baiu front event of 2 June 2006, the data were separated into the following categories: (a) convective rainfall (CV), (b) stratiform rainfall before the CV (Before-CV), and (c) stratiform rainfall after the CV (After-CV) as shown in Table 1 and Fig 2. The Classification was based on; (1) the existence of the bright band (BB); (2) the existence of the region that was more than 45dBZ; (3) vertical structure of radar polarimetric parameters (Z, ZDR, and ρ_{HV}) and Doppler spectrum.

TABLE 1 List of the rainfall events period that are classified into three rainfall type.

Rainfall Type	Rain event (JST)
Before-CV	07:30 – 09:59
CV	10:00 – 10:30
After-CV	10:31 – 11:59

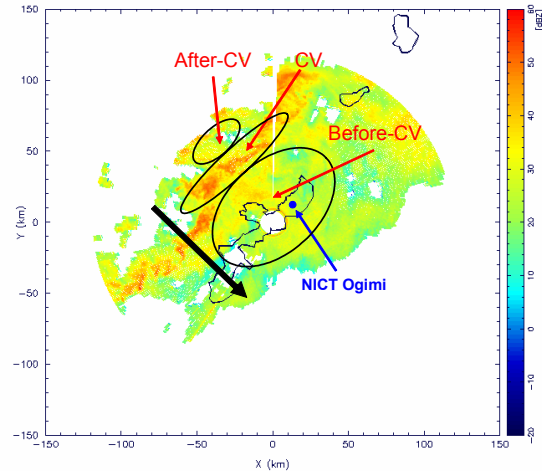


Fig. 2 PPI display of radar reflectivity factor at 8:54 JST. The elevation angle is 1.8°. The black arrow shows the direction of movement of the rain-band at the SE. The solid blue dot indicates the location of the 400-MHz WPR and the two disdrometers.

3.3 DSD characteristics of rainfall parameters

We focused on the differences in DSD parameters between the 'Before-CV' and the 'After-CV' rain events. From an examination of the ground-based

measurements of the DSD observed by the 2DVD, we found that the size distributions of the ‘Before-CV’ rain were generally broader and less peaked than the ‘After-CV’ rain events as shown in Fig. 3. Fig. 4 shows the relationship between the radar reflectivity (Z) and the mass weighted drop diameter (D_m). Fig. 5 shows the relationship between the radar reflectivity and the normalized number concentration (N_0^*). The values of D_m were larger during the ‘Before-CV’ rain than in the ‘After-CV’ rain. On the other hand, the values of N_0^* were larger during the ‘After-CV’ rain than in the ‘Before-CV’ rain. As a result, the $Z-D_m$ and $Z-N_0^*$ relationships for the two stratiform periods differ.

Next, we focused on the vertical rainfall structures to explain the differences in the ground-based measurements of the DSD during the two stratiform periods of rain. Fig. 6 shows the vertical profile of the differential reflectivity (ZDR) observed by COBRA. The values of ZDR were typically larger during the ‘Before-CV’ rain than in the ‘After-CV’ rain. This result was confirmed from the radar ZDR estimated from the 400-MHz WPR data (as shown in Fig. 7). In Fig. 6, the location of the bright band (BB) in the ‘Before-CV’ period was found to be lower than the BB location during ‘After-CV’ period. This result was confirmed by the Doppler spectrum observed by the 400-MHz WPR (as shown in Fig. 8).

In summary, the differences in the ground-based DSD depend on the differences in the vertical profile of the differential reflectivity and the location of the bright band.

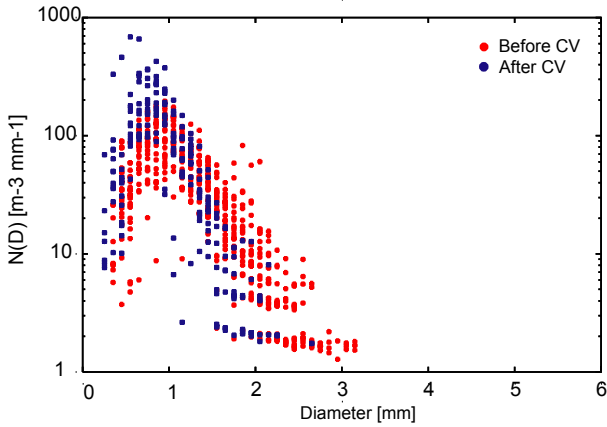


Fig. 3 Drop size distribution in each rainfall event, ‘Before-CV’ and ‘After-CV’ for $1\text{mm/h} < R < 1.5\text{mm/h}$. R is rainfall intensity. All samples of 1 minute duration.

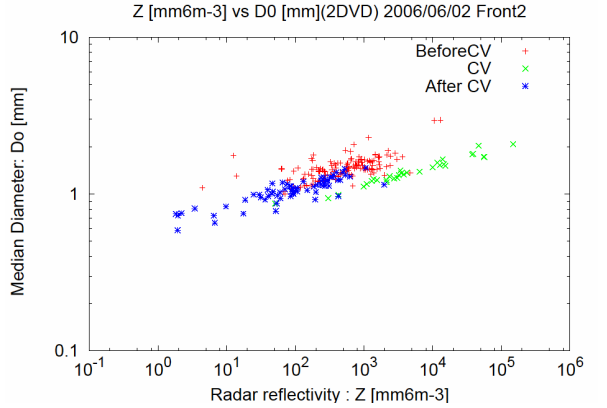


Fig. 4 The relationship between the radar reflectivity (Z) and the mass weighted drop diameter (D_m).

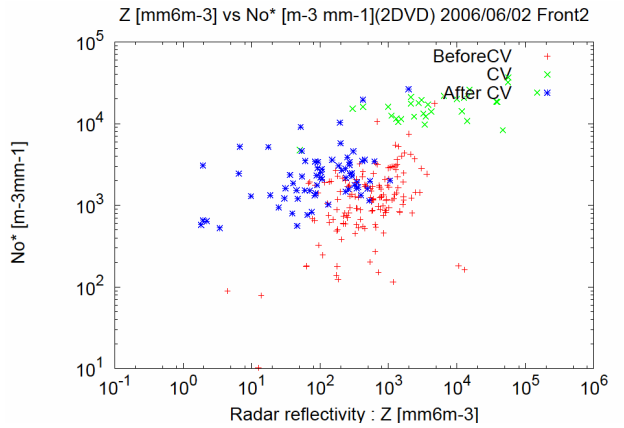


Fig. 5 The relationship between the radar reflectivity (Z) and the normalized number concentration (N_0^*).

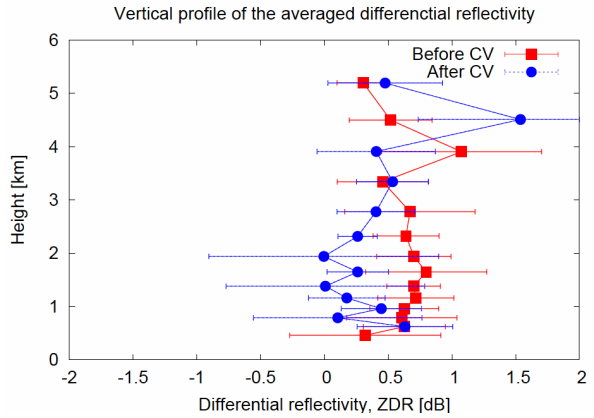


Fig. 6 Vertical profile of the differential reflectivity (ZDR) observed by COBRA during the ‘Before-CV’ and ‘After-CV’ rainfall. The dot is the averaged value. The error bar is the standard deviation.

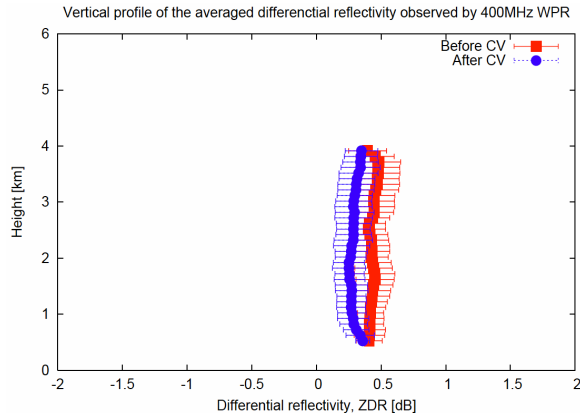


Fig. 7 Vertical profile of the differential reflectivity (ZDR) below the melting layer estimated from the 400-MHz WPR data (Y. Kitamura et al., 2003). The dot is the averaged value. The error bar is the standard deviation.

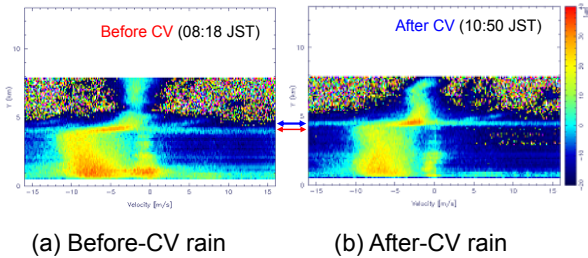


Fig. 8 Doppler spectrum observed by the 400-MHz WPR. The red arrow shows a BB height of 'Before-CV' rain. The blue arrow shows a BB height of 'After-CV' rain.

4. SUMMARY

Measurements from intensive field observations of subtropical precipitation using COBRA, 400-MHz WPR, and two types of ground-based disdrometer were used to analyze the vertical characteristics of rainfall with rainfall type. To characterize the vertical variations in the rainfall, the data were separated into the following categories: (a) convective rainfall (CV), (b) stratiform rainfall before the CV (Before-CV), and (c) stratiform rainfall after the CV (After-CV).

The results show that the ground-based DSD of the 'Before-CV' rain are generally broader and less peaked than the 'After-CV' rain events. As a consequence, the $Z-D_m$ and $Z-N_0^*$ relationships for the two stratiform periods differ. Next, we focused on the vertical rainfall structures to explain the differences in the ground-based measurements. We found that the differences in the ground-based DSD depend on the differences in the vertical profile of the differential reflectivity and on the location of the bright band.

Using the COBRA and the 400-MHz WPR data, a future objective is to develop a model for the vertical variation in the drop size distribution for stratiform and convective rain types.

5. ACKNOWLEDGMENT

This study was supported by the Core Research for Evolutional Science and Technology (CREST) project, of the Japan Science and Technology Agency (JST).

6. REFERENCES

- T. Iguchi, H. Hanado, N. Takahashi, S. Kobayashi, and S. Satoh: The dual-frequency precipitation radar for the GPM core satellite. *Proc. IGARSS 2003, Toulouse*.
- C. Kummerow, Y. Hong, W. S. Olson, S. Yang, R. F. Adler, J. McCollum, R. Ferraro, G. Petty, D.-B. Shin, and T. T. Wilheit: The Evolution of the Goddard Profiling Algorithm(GPROF) for Rainfall Estimation from Passive Microwave Sensors. *J. Appl. Meteor.*, Vol. 40, pp.1801-1820, 2001.
- K. Aonashi, and G. Liu: Passive microwave precipitation retrievals using TMI during the Baiu preiod of 1999. Part I: ALgorithm description and validation. *J. Appl. Meteor.*, Vol. 39, pp.2024-2037, 2000.
- K. Nakagawa, Y. Kitamura, K. Iwanami, H. Hanado, K. Okamoto, 2005 : Field Campaign of Observing Precipitation in the 2004 Rainy Season of Okinawa, Japan. *Proc. IGARSS, IEEE*, 109-116
- K. Nakagawa, H. Hanado, S. Satoh, N. Takahashi, T. Iguchi and K. Fukutani, 2003: Development of a new C-band bistatic polarimetric radar and observation of typhoon events. *Proc. 31st Conf Radar Meteor, AMS*, vol. 2, 863-866.
- T. Adachi, Y. Masuda, and S. Fujii, 2001; Development of a 400MHz Wind Profiler in Okinawa. *The third International Symposium on Asian Monsoon System (IMAS3)*, 309-313.
- K. Wakasugi, S. Fukao, S. Kato, A. Mizutani, and Matsu, 1986: A direct method for deriving drop-size distribution and vertical air velocities from VHF Doppler radar spectra. *J. Atmosos. Ocean. Tech.*, 3, 623-629.
- T. Sato, H. Doji, H. Iwai, I. Kimura, S. Fuako, M. Yamoto, T. Tsuda, and S. Kato, 1990: Computer processing for deriving drop-size distribution and vertical air velocities from VHF Doppler radar spectra. *Radio Science*, 5, 961-973.
- T. Kobayashi and A. Adachi, 2005: Retrieval of Arbitrarily Shaped Raindrop Size Distributions from Wind Profiler Measurements. *J. Atmosos. Ocean. Tech.*, 4, 433-442.
- Y. Kitamura, K. Nakagawa, S. Sekizawa, H. Hanado, N. Takahashi, and T. Iguchi, 2005: Vertical profile of raindrop size distribution by using 400MHz Wind Profiler in stratiform rainfall. *Proc. 32nd Conf Radar Meteor, AMS*.
- C. W. Ulbrich, 1983: Natural variation in the analytical form of raindrop size distributions. *J. Climate Appl. Meteor.*, 22, 1764-1775.
- T. Kozu and K. Nakamura, 1991: Rainfall parameter estimation from dual radar measurements combining reflectivity profile and path-integrated attenuation. *J. Atmosos. Ocean. Tech.*, 8, 259-270.